Joint OSC Receiver for Evolved GSM/EDGE Systems

Daniele Molteni and Monica Nicoli, *Member, IEEE*

***Abstract*—This paper is focused on evolved GSM/EDGE systems complying to the new feature Voice services over Adaptive Multi-user channels on One Slot (VAMOS), recently introduced in the 3GPP GSM/EDGE radio access network (GERAN) standard. VAMOS enables the transmission of two GSM voice streams on the same radio resource through the so called Orthogonal Sub Channel (OSC) multiple access technique which aims at doubling the number of users served by a cell. When adopting this feature, the GSM network experiences a mixture of in-cell and out-of-cell interference which has to be handled by advanced receivers with interference rejection capabilities. In this paper, a novel two-stage receiver is proposed and tested for the uplink of GSM VAMOS systems. The new scheme combines a pre-filtering stage for out-of-cell interference mitigation with a multi-user detector (MUD) for joint equalization of the two multiplexed OSC streams. The approach is suited for either single-antenna or multi-antenna base stations and can accommodate multiple filters for each user to cope with complex multipath propagation scenarios. The new solution is compared with other existing interference cancellation techniques here applied to the specific OSC scenario. Numerical results show significant performance gains in realistic multi-cell simulated scenarios.**

***Index Terms*—Cellular networks, GSM, GERAN, OSC, VAMOS, interference cancellation, equalization, multiuser detection, multiple antennas, orthogonal sub channels.**

I. Introduction

THE Global System for Mobile communications (GSM) is the world's most widely used mobile wireless system, with more than 4 billions subscriptions all over the world covering around 80% of the global market [1]. Though the European GSM market has been saturating recently due to the advent of 3G networks, on a worldwide basis the GSM traffic demand is still increasing thanks to the rapid growth of emerging markets [2]. At the same time, in networks with phasing out GSM services, there is the need to liberate spectrum resources in the 900 and 1800 MHz bands for accommodating more 3G-4G users (spectrum refarming). This trend pushed in the last few years the operators to find new ways to optimize the network planning and improve the spectral efficiency, limiting as much as possible the impact on the existing hardware equipment.

Manuscript received December 29, 2011; revised July 11 and December 10, 2012; accepted February 2, 2013. The associate editor coordinating the review of this paper and approving it for publication was S. Blostein.

D. Molteni was with the Dipartimento di Elettronica e Informazione (DEI), Politecnico di Milano, I-20133 Milan, Italy. He is now with Schlumberger Gould Research Center, High Cross, Madingley Road, CB3 0EL, Cambridge, United Kingdom (e-mail: molteni.daniele@gmail.com).

M. Nicoli is with the Dipartimento di Elettronica, Informazione e Bioingegneria (DEIB), Politecnico di Milano, I-20133 Milan, Italy (e-mail: monica.nicoli@ polimi.it).

This work has been partially supported by Nokia Siemens Networks, Cinisello Balsamo, Milano, Italy.

Digital Object Identifier 10.1109/TWC.2013.050613.112296

A well known approach for increasing the number of served users per unit area is the reduction of the reuse factor which implies however a higher co-cell interference. In 2009 implementation guidelines for new GSM handsets with higher interference mitigation capabilities have been provided by the Third Generation Partnership Project (3GPP) through the definition of Downlink Advanced Receiver Performance (DARP) phase I-II requirements [3]. New DARP compliant handsets have been released on the market based on proprietary implementations of the so called Single/Double/Multiple Antenna Interference Cancellation (SAIC/DAIC/MAIC) algorithms [4]-[8]. A common approach is to use derotation to express the received GSM signal as a complex filtering of a real-valued modulation and then exploit the non-circularity property for boosting interference filtering [7] [8]. The received signal is mapped onto a virtual antenna-array domain that comprises all the available signal dimensions, namely the in-phase/quadrature (I/Q) components, multiple antennas (if available) and time oversampling. In the new multi-dimensional and hybrid (space, time, I/Q) real-valued domain, the transmitted signal is typically confined to a subspace and can be separated from impairments by spatial filtering (or beamforming).

Relying on the improved robustness to interference of the new GSM mobiles, recently the GSM/EDGE Radio Access Network (GERAN) group introduced the Voice services over Adaptive Multi-user channels on One Slot (VAMOS) [6], discussed in the work item Multiple Users Reusing One Slot (MUROS). This feature is part of the evolved EDGE features of the 3GPP GERAN standard - Release 9 [9]. VAMOS enables the transmission of two GSM voice streams over the same channel through the so called Orthogonal Sub Channel (OSC) multiplexing technique [10] [11]. Recalling that GSM employs Gaussian minimum shift keying (GMSK) modulation, which can be well approximated by a filtered binary phase shift keying (BPSK) modulation [7], in OSC systems two GSM streams are transmitted on the same carrier as two superimposed phase-shifted BPSK signals and they are separated at the receiver by selective filtering. In downlink (DL), the base station (BS) exploits a subset of the 8-PSK constellation of the EDGE standard to generate the two GMSK streams, phase-shifted by $\pi/2$, and each mobile station (MS) recovers the desired sequence using a DARP receiver. Power control can be achieved adopting the optional feature α-QPSK [6]. In uplink (UL), two MSs transmit GMSK modulated signals on the same channel and the BS recovers the transmitted sequences by an array processing algorithm for interference filtering. For channel estimation over OSC links, new training sequences (TSC) have been introduced with low

cross-correlation to the standard compliant ones [12]. New challenges are resource allocation policies for optimization of user pairing, multi-cell interference management (see, e.g., [13] for 4G networks) and physical-layer algorithms for mitigation of the in-cell impairments.

A. Related Works

The success of VAMOS multiplexing relies on the interference reduction capabilities of the receiver. Interference filtering techniques have been widely investigated for conventional 2G scenarios (see, e.g., [14]-[16]), but the literature is still poor on the new OSC application. A SAIC receiver explicitly derived for the VAMOS downlink environment has been proposed in [17]. SAIC and MAIC algorithms have been originally developed for legacy GSM systems with, respectively, single-antenna and multi-antenna receivers [5], [7], [18]-[23]. For GSM systems compliant with DARP specifications the most affirmed solution so far has been a single-user receiver with a pre-filter to reduce the out-of-cell interference and an equalizer (either linear or non-linear) for recovering the data stream of the desired user. Such solutions can be considered also for OSC systems, using a separate SAIC/MAIC filter for each OSC user; the advantage would be the moderate computational complexity. A first assessment has been presented in [19], where the SAIC solution [7] has been tested on a noise and interference limited OSC DL scenario, using a single-user SAIC filter for each OSC user.

Differently from conventional single-user filter-based solutions, in multi-user detection (MUD) the mutual interference between the in-cell users is optimally handled by a simultaneous detection of the users' signals [24]. While joint maximum likelihood sequence estimation (JMLSE) has a prohibitive computational cost that increases exponentially with the number of users [25] [26], a good performance/complexity trade-off is provided by reduced-state trellis-based joint detection [27]. A joint reduced-state sequence detector with delayed decision feedback has been proposed in [28] for MIMO systems with application to the EDGE standard. A suboptimal approach, which further lowers the complexity, is Successive Interference Cancellation (SIC) [19] [29], based on sequential decoding and cancellation of the detected users' streams from the received signals. This solution has been recently considered by 3GPP as a possible receiving strategy for OSC-GERAN scenarios [11].

The problem of resource allocation and user pairing in GSM-OSC systems has been studied in [30] while the capacity gain provided by the OSC feature has been analyzed in [31]. The work [32] focused on the DL scenario, particularly on the performance of channel estimation and the impact of power imbalance between the OSC users.

B. Original Contribution

In this work we propose a two-stage receiving architecture for the UL of a GSM VAMOS system. The proposed scheme, specifically designed for the OSC scenario and referred to as joint OSC receiver (JOR), combines a pre-filtering stage for out-of-cell interference mitigation with a MUD stage for joint detection of the two multiplexed OSC streams. As no information of the out-of-cell users is available at the receiver, the out-of-cell interference is treated as noise correlated over the space-time domain and uncorrelated over the time symbols. On the other hand, intra-cell OSC users are handled coherently using the knowledge of the two channel impulse responses obtained from the training sequences.

Unlike existing SAIC/MAIC receivers, in the JOR solution the filters of the first stage are *jointly* designed for the two OSC users so as to minimize the *out-of-cell* impairment while preserving the two in-cell multiplexed signals. Processing applies to the received signals mapped onto the real-valued equivalent domain and it is suited for both single and multiple antenna systems. Optimal filters are derived by maximizing the Signal to Interference plus Noise Ratio (SINR) of each OSC user where the interference is represented by the out-of-cell impairment only (not the in-cell one). This allows a more effective pre-filtering, as all the available degrees of freedom in the filters' design are used to reject the dominant out-of-cell interferer, while the in-cell interference between the OSC users can be handled in the second stage by either linear or non-linear MUD [24].

An alternative two-stage receiver has been proposed in [20] for interference mitigation in a single-user GSM context. Although the two methods have in common a two-stage structure, the approach herein proposed aims to detect the two users simultaneously, it is multi-antenna and is cast for the new OSC modulation scheme. A similar architecture has been proposed in [28] for legacy EDGE systems, where the filter design follows the MMSE criterion and decision feedback is employed as a computationally efficient solution. The analysis in [28], however, does not consider the application to the VAMOS context.

A preliminary study of the JOR architecture has been presented in [33]. In this work, we provide a more in-depth analysis, with optimal filter derivation and validation on realistic GSM-OSC multi-cell scenarios. The architecture is extended to accommodate multiple filters for each OSC user, in order to improve the data detection performance in complex cellular scenarios. Multiple filters are indeed needed in rich scattering environments and/or in high-SINR regime, where the performance of the (one-dimensional) JOR is limited by the bias due to the prefilter which performs a projection of the received signal onto the subspace associated with the dominant channel component. Performance improvement provided by multiple filters comes at the price of an increased computational complexity; the number of filters has to be evaluated as trade-off between detection performance and computational complexity, taking into account the specific propagation environment and the hardware/software constraints.

II. Signal Model

A. Received Signal

We consider the uplink of a GERAN system with OSC feature as defined in [11]. The cellular layout and the communication system structure are shown in Fig. 1. Two MSs transmit voice streams towards a common BS through the same radio resource (i.e., carrier frequency and time slot),

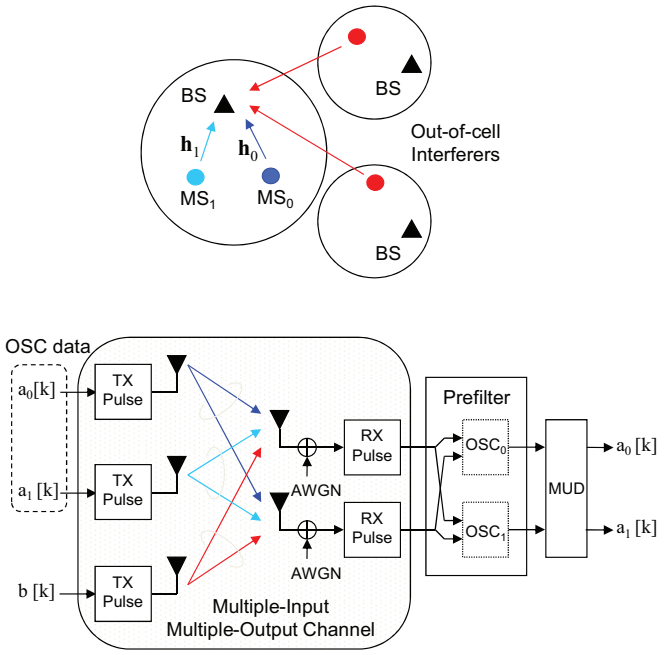

Fig. 1. GSM-OSC uplink scenario: cell layout and communication system structure. The two MSs in the cell share the same frequency and time slot. The proposed joint OSC receiver applies a prefilter to mitigate the out-of-cell interferer and a multiuser detector to recover the sequences of the desired users.

using a standard compliant GMSK modulation. Transmission is supposed to be impaired by V out-of-cell interferers. The BS is equipped with $N_{\rm R}$ receiving antennas while each MS has only one transmitting antenna. Receiving antennas are assumed to be sufficiently spaced apart so that the signals at different antennas can be considered as uncorrelated with each other.

According to the standard [34], at each MS the sequence of information bearing bits is divided into classes of data that are convolutionally and differentially encoded, then mapped over a number of bursts according to the selected channel coding scheme [9]. As shown in Fig. 2, each burst consists of $K = 148$ symbols made up of: 114 data symbols (arranged in two semi-bursts of $K_{\rm d} = 57$ symbols each), 8 guard symbols and a TSC of $K_{\rm tsc} = 26$ symbols. The TSCs of the OSC users are known at the BS while no information is available on the out-of-cell interferers.

Let us consider a single burst, the kth transmitted bit, $k = 1, \ldots, K$, is denoted as $a_i[k] \in \{\pm 1\}$ for the ith OSC user with $i = 0$ or $i = 1$, and $b_v[k] \in \{\pm 1\}$ for the vth out-of-cell interferer with $v = 1, \ldots, V$. Following the GMSK linearized model [34], the complex base-band signals at the output of the receiver front-end filter are here arranged into the $N_{\rm R} \times 1$ vector:

$$\bar{\mathbf{y}}(t) = \sum_{i=0}^{1}\sum_{k=1}^{K} \bar{\mathbf{h}}_i(t - kT)\; j^k\; a_i[k] \; + \; + \sum_{v=1}^{V}\sum_{k=1}^{K} \bar{\mathbf{h}}_{{\rm I},v}(t - kT)\; j^k\; b_v[k] \; + \; \bar{\mathbf{n}}_{\rm bn}(t), \qquad (1)$$

where $1/T$ is the baud rate, the $N_{\rm R} \times 1$ vector $\bar{\mathbf{h}}_i(t)$ collects the $N_{\rm R}$ channel impulse responses at time t for the ith OSC user while $\bar{\mathbf{h}}_{{\rm I},v}(t)$ refers to the channel of the vth out-of-cell interferer. Here the channels are modelled according to the block-fading assumption (same fading response within a burst), and their responses comprise the pulse shaping filter (i.e., the linearized GMSK pulse waveform), the time-varying multipath fading effects, the front-end filter and the phase offset between the OSC users. The complex term j^k is the periodic rotation of the GMSK equivalent linear representation [34]. The vector $\bar{\mathbf{n}}_{\rm bn}(t)$ denotes the background noise colored by the front-end filter, with covariance $\mathrm{E}[\bar{\mathbf{n}}_{\rm bn}(t)\bar{\mathbf{n}}_{\rm bn}^{\rm H}(t+\tau)] = \sigma_{\rm bn}^2 \mathbf{I}_{N_{\rm R}} G(\tau)$ where $G(\tau)$ is the autocorrelation of the front-end filter response and $\sigma_{\rm bn}^2$ is the power spectral density of the additive white Gaussian noise at the receiver.

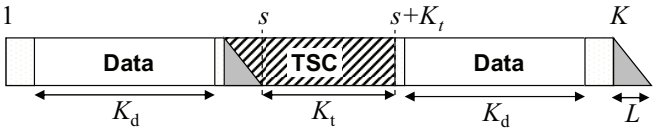

Fig. 2. GSM burst structure.

B. Equivalent Real-valued Discrete-time Model

To ease interference cancellation we first convert (1) into an equivalent real-valued discrete-time signal by sampling, derotation and separation of the I/Q components, following the guidelines in [8]. The transformation, here adapted and detailed for the specific GSM-OSC scenario, provides the signal model that will be used in Section III for the design of the filters for interference mitigation.

The complex-valued signal (1) is first oversampled with frequency $2/T$[1]. The $2N_{\rm R}$ samples associated with the kth symbol time are gathered into the *hybrid space-time* (ST) vector $\bar{\mathbf{y}}_s[k] = [\bar{\mathbf{y}}^{\rm T}(kT), \bar{\mathbf{y}}^{\rm T}(kT + T/2)]^{\rm T}$, modelled as

$$\bar{\mathbf{y}}_s[k] = \bar{\mathbf{H}}_{s,0}[k]\mathbf{a}_0[k] + \bar{\mathbf{H}}_{s,1}[k]\mathbf{a}_1[k] + \mathbf{n}_s[k], \qquad (2)$$

where $\mathbf{a}_i[k] = [a_i[k] \cdots a_i[k-L]]^{\rm T}$ collects the last $L+1$ symbols of the ith OSC user, L denotes the channel order and $\mathbf{n}_s[k]$ represents the sampled noise plus out-of-cell interference. The GMSK periodic symbol rotation has been included in the time-varying discrete-time channel impulse response $\bar{\mathbf{H}}_{s,i}[k]$, defined for the ith OSC user as

$$\bar{\mathbf{H}}_{s,i}[k] = \begin{bmatrix} j^k\bar{\mathbf{h}}_i[0] & j^{k-1}\bar{\mathbf{h}}_i[1] & \cdots & j^{k-L}\bar{\mathbf{h}}_i[L] \\ j^k\bar{\mathbf{h}}_i[\frac{1}{2}] & j^{k-1}\bar{\mathbf{h}}_i[1+\frac{1}{2}] & \cdots & j^{k-L}\bar{\mathbf{h}}_i[L+\frac{1}{2}] \end{bmatrix}, \qquad (3)$$

where $\bar{\mathbf{h}}_i[\ell] = \bar{\mathbf{h}}_i(\ell T)$ and $\bar{\mathbf{h}}_i[\ell + 1/2] = \bar{\mathbf{h}}_i((\ell + 1/2)T)$, for $\ell = 0, 1, \ldots, L$, denote the two polyphase channel components. The GMSK linearized signal (2) is then converted into an equivalent bipolar modulated stream by derotation. The derotated signal is obtained as $\bar{\mathbf{y}}_d[k] = \mathbf{J}[k]\bar{\mathbf{y}}_s[k]$ through the $2N_{\rm R} \times 2N_{\rm R}$ derotation matrix $\mathbf{J}[k] = \mathrm{diag}\left\{j^{-k}, j^{-(k+1/2)}\right\} \otimes \mathbf{I}_{N_{\rm R}}$, with $\otimes$ denoting the Kronecker product. The resulting complex-valued signal is the sum of two mutually-interfering

[1]For the GSM signal bandwidth, an oversampling factor of 2 can be considered enough to represent the user signal without distortion and exploit temporal diversity for users' signal separation; no significant gain has been observed by further increasing the sampling frequency.

BPSK signals filtered by time-invariant complex channels:

$$\bar{\mathbf{y}}_d[k] = \bar{\mathbf{H}}_{d,0}\mathbf{a}_0[k] + \bar{\mathbf{H}}_{d,1}\mathbf{a}_1[k] + \mathbf{n}_d[k], \tag{4}$$

where $\bar{\mathbf{H}}_{d,i}$ represents, for user $i \in \{0,1\}$, the complex-valued derotated channel response which is no more dependent on the time index k:

$$\bar{\mathbf{H}}_{d,i} = \mathbf{J}[k]\bar{\mathbf{H}}_{s,i}[k] = \begin{bmatrix} \bar{\mathbf{h}}_i[0] & j^{-1}\bar{\mathbf{h}}_i[1] & \cdots & j^{-L}\bar{\mathbf{h}}_i[L] \\ j^{-\frac{1}{2}}\bar{\mathbf{h}}_i[\frac{1}{2}] & j^{-\frac{3}{2}}\bar{\mathbf{h}}_i[1+\frac{1}{2}] & \cdots & j^{-L-\frac{1}{2}}\bar{\mathbf{h}}_i[L+\frac{1}{2}] \end{bmatrix}. \tag{5}$$

Next, we separate and rearrange the real and imaginary parts of (4) into the $4N_{\mathrm{R}} \times 1$ real-valued vector:

$$\mathbf{y}[k] = \begin{bmatrix} \mathrm{Re}\{\bar{\mathbf{y}}_d[k]\} \\ \mathrm{Im}\{\bar{\mathbf{y}}_d[k]\} \end{bmatrix} = \mathbf{H}_0\mathbf{a}_0[k] + \mathbf{H}_1\mathbf{a}_1[k] + \mathbf{n}[k], \tag{6}$$

where the ith channel response is now represented by the $4N_{\mathrm{R}} \times (L+1)$ real-valued matrix $\mathbf{H}_i = [\mathrm{Re}\{\bar{\mathbf{H}}_{d,i}^{\mathrm{T}}\}, \mathrm{Im}\{\bar{\mathbf{H}}_{d,i}^{\mathrm{T}}\}]^{\mathrm{T}}$ and the noise term by the $4N_{\mathrm{R}} \times 1$ vector $\mathbf{n}[k] = [\mathrm{Re}\{\mathbf{n}_d^{\mathrm{T}}[k]\}, \mathrm{Im}\{\mathbf{n}_d^{\mathrm{T}}[k]\}]^{\mathrm{T}}$.

Finally, we collect the samples of the whole burst into the $4N_{\mathrm{R}} \times (K+L)$ matrix:

$$\mathbf{Y} = [\mathbf{y}[1] \cdots \mathbf{y}[K+L]] = \mathbf{H}_0\mathbf{A}_0 + \mathbf{H}_1\mathbf{A}_1 + \mathbf{N}, \tag{7}$$

using $\mathbf{A}_i = [\mathbf{a}_i[1] \cdots \mathbf{a}_i[K+L]]$ to denote the convolution matrix for the ith OSC user symbols and $\mathbf{N} = [\mathbf{n}[1], ..., \mathbf{n}[K+L]]$ for collecting the samples of the overall correlated impairments (out-of-cell interference and background noise). Correlation depends on the choice of the front-end filter and of the oversampling factor.

C. Training Signals

The filters for interference mitigation and the channel impulse responses for data detection will be derived, as described in the following section, using the knowledge of the two TSCs of length K_{tsc}. The $4N_{\mathrm{R}} \times K_{\mathrm{t}}$ midamble signals extracted from (6) can be written as:

$$\mathbf{Y}_{\mathrm{t}} = [\mathbf{y}[s+1], ..., \mathbf{y}[s+K_{\mathrm{t}}]] \tag{8}$$

$$= [\mathbf{H}_0, \mathbf{H}_1] \begin{bmatrix} \mathbf{A}_{\mathrm{t},0} \\ \mathbf{A}_{\mathrm{t},1} \end{bmatrix} + \mathbf{N}_{\mathrm{t}} = \mathbf{H}\mathbf{A}_{\mathrm{t}} + \mathbf{N}_{\mathrm{t}}. \tag{9}$$

where s denotes the index of the first useful bit of the midamble (after a first tail of L bits affected by the ISI from the first semi-burst, see Fig. 2), $K_{\mathrm{t}} = K_{\mathrm{tsc}} - L$ is the total number of useful training bits, $\mathbf{A}_{\mathrm{t},i}$ is the $(L+1) \times K_{\mathrm{t}}$ convolution matrix for the training sequence of the ith OSC user, $\mathbf{A}_{\mathrm{t}} = [\mathbf{A}_{\mathrm{t},0}^{\mathrm{T}}\ \mathbf{A}_{\mathrm{t},1}^{\mathrm{T}}]^{\mathrm{T}}$ is the multi-user matrix, and $\mathbf{N}_{\mathrm{t}}$ represents the noise plus out-of-cell interference contribution in the midamble section of the burst. From signals (8), we can easily compute the *joint* least squares (LS) estimate of the two OSC user channels as $[\hat{\mathbf{H}}_0, \hat{\mathbf{H}}_1] = \mathbf{R}_{ya}\mathbf{R}_{aa}^{-1}$ with $\mathbf{R}_{ya} = \mathbf{Y}_{\mathrm{t}}\mathbf{A}_{\mathrm{t}}^{\mathrm{T}}$ and $\mathbf{R}_{aa} = \mathbf{A}_{\mathrm{t}}\mathbf{A}_{\mathrm{t}}^{\mathrm{T}}$.

III. Joint OSC Receiver (JOR)

A. Receiver Architecture

For GSM-OSC systems we propose a receiving scheme that combines a front-end space-time filtering stage with a MUD stage as described in Fig. 1. The first stage aims at reducing the out-of-cell interference *jointly* for the two OSC users by means of two linear filters $\{\mathbf{w}_0, \mathbf{w}_1\}$. The ith filter, $i \in \{0,1\}$, combines $4N_{\mathrm{R}}$ samples - per symbol time - of the received signal (6) to obtain the data stream of the ith OSC user:

$$\begin{cases} \mathbf{y}_{w,0}^{\mathrm{T}} = \mathbf{w}_0^{\mathrm{T}}\mathbf{Y} = \mathbf{h}_{w,00}^{\mathrm{T}}\mathbf{A}_0 + \mathbf{h}_{w,01}^{\mathrm{T}}\mathbf{A}_1 + \mathbf{n}_0^{\mathrm{T}} \\ \mathbf{y}_{w,1}^{\mathrm{T}} = \mathbf{w}_1^{\mathrm{T}}\mathbf{Y} = \mathbf{h}_{w,10}^{\mathrm{T}}\mathbf{A}_0 + \mathbf{h}_{w,11}^{\mathrm{T}}\mathbf{A}_1 + \mathbf{n}_1^{\mathrm{T}} \end{cases}. \tag{10}$$

The $4N_{\mathrm{R}} \times 1$ filter coefficients $\{\mathbf{w}_0, \mathbf{w}_1\}$ and the related $(L+1) \times 1$ filtered channels $\{\mathbf{h}_{w,00}, \mathbf{h}_{w,11}\}$ are derived from the training signals (8) in such a way so as to minimize the contribution of the out-of-cell interference, as described in Section III-B. Filtered signals are then fed to the second stage that performs a temporal filtering for detection of the two OSC sequences $\{a_0[k], a_1[k]\}$, namely a joint detection aiming at reducing the effects of the mutual interference due to the cross channels $\mathbf{h}_{w,01}^{\mathrm{T}} = \mathbf{w}_0^{\mathrm{T}}\mathbf{H}_1$ and $\mathbf{h}_{w,10}^{\mathrm{T}} = \mathbf{w}_1^{\mathrm{T}}\mathbf{H}_0$, and the residual noise or interference $\mathbf{n}_i = \mathbf{w}_i^{\mathrm{T}}\mathbf{N}$, as described in Section III-C.

B. Prefilter Design

The criterion for derivation of $\{\mathbf{w}_i, \mathbf{h}_{w,ii}\}$ for user $i \in \{0,1\}$, is the maximization of the SINR evaluated on the training signal (8) after prefiltering, SINR_i, considering as interference only the *out-of-cell* impairment:

$$\left\{\hat{\mathbf{w}}_i, \hat{\mathbf{h}}_{w,ii}\right\} = \arg \max_{\mathbf{w}_i, \mathbf{h}_{w,ii}} \mathrm{SINR}_i. \tag{11}$$

We define the SINR on the real-valued signal received within a single burst, as defined in Sec. II-B. Linear prefiltering accounts for the spatial dimension (multiple antennas), polyphase and I/Q components; extension to include the temporal dimension -spanning over multiple symbol times- can be performed as in [21]. Multi-burst signals [35] are not considered here as the frequency hopping feature is enabled for the OSC environment [6]; frequency hopping makes the channel and the interference space-time structure change on a burst by burst basis, thus requiring the computation of the filter coefficients and channel responses for each burst.

For $i = 0$ (and similarly for $i = 1$), the SINR at the output of the prefilter $\mathbf{w}_0$ is defined as:

$$\mathrm{SINR}_0 = \frac{\left\|\mathbf{h}_{w,00}^{\mathrm{T}}\mathbf{A}_{\mathrm{t},0}\right\|^2}{\left\|\mathbf{w}_0^{\mathrm{T}}\left(\mathbf{Y}_{\mathrm{t}} - \mathbf{H}_1\mathbf{A}_{\mathrm{t},1} - \mathbf{H}_0\mathbf{A}_{\mathrm{t},0}\right)\right\|^2} \tag{12}$$

$$= \frac{\left\|\mathbf{h}_{w,00}^{\mathrm{T}}\mathbf{A}_{\mathrm{t},0}\right\|^2}{\left\|\mathbf{w}_0^{\mathrm{T}}\mathbf{Y}_{\mathrm{t}} - \mathbf{w}_0^{\mathrm{T}}\mathbf{H}_1\mathbf{A}_{\mathrm{t},1} - \mathbf{h}_{w,00}^{\mathrm{T}}\mathbf{A}_{\mathrm{t},0}\right\|^2}, \tag{13}$$

where $\|\cdot\|^2$ denotes the Frobenius norm of the argument vector. The numerator of (12) represents the power of the desired user signal at the pre-filtering output, while the denominator is the power of filtered interference and background noise[1]. We recall that the aim of filtering here is the minimization of the *out-of-cell* impairment only; all the degrees of freedom for filtering are used for the minimization of the out-of-cell interference, while the in-cell one will be optimally handled

[1]The SINR has been defined similarly to [16], extending the model to the herein considered dual-user scenario.

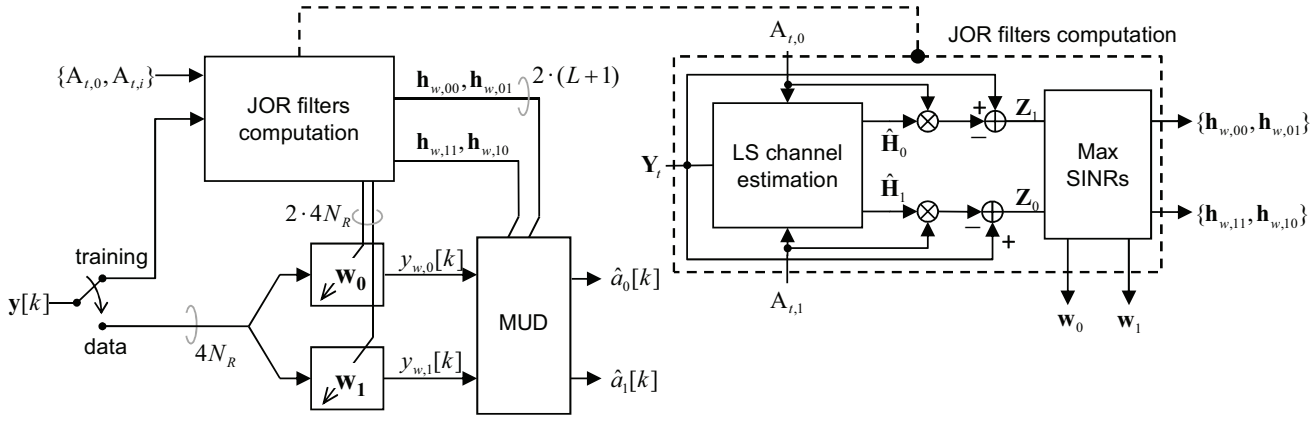

Fig. 3. JOR structure: the filters $\{\mathbf{w}_0, \mathbf{w}_1\}$ are designed to provide the maximum SINR for each OSC user over the signals $\{\mathbf{Z}_0, \mathbf{Z}_1\}$ for the 0th and 1st user respectively. The filtered signals and related channel responses are then used by the MUD block to recover the transmitted sequences.

by MUD. Hence the denominator does not include the signal generated by user 1 which is removed from the received data $\mathbf{Y}_{\rm t}$. This optimization requires a joint processing for the two OSC users, as the filters for one user must be calculated taking into account the channels of both users.

For reconstruction of the interfering user sequence in the denominator of (12) we choose to employ the joint LS estimate $\hat{\mathbf{H}}_1$ (see Sec. II-C), which is available from training data, thus obtaining:

$$\mathrm{SINR}_0 = \frac{\left\|\mathbf{h}_{w,00}^{\mathrm{T}}\mathbf{A}_{\mathrm{t},0}\right\|^2}{\left\|\mathbf{w}_0^{\mathrm{T}}\mathbf{Z}_0 - \mathbf{h}_{w,00}^{\mathrm{T}}\mathbf{A}_{\mathrm{t},0}\right\|^2}, \tag{14}$$

where $\mathbf{Z}_0 = \mathbf{Y}_{\rm t} - \hat{\mathbf{H}}_1\mathbf{A}_{\mathrm{t},1}$. The maximization of (14) can be obtained following the approach in [16] applied to the received signal after user 1 cancellation, $\mathbf{Z}_0$, yielding the solution:

$$\mathbf{w}_0 = \mathbf{R}_{zz,0}^{-1}\mathbf{R}_{za,0}\hat{\mathbf{h}}_{w,00}, \tag{15}$$

$$\hat{\mathbf{h}}_{w,00} = \mathbf{R}_{aa,0}^{-\frac{1}{2}}\,\mathrm{eig\,max}\left(\mathbf{R}_{aa,0}^{-\frac{\mathrm{T}}{2}}\mathbf{R}_{az,0}\mathbf{R}_{zz,0}^{-1}\mathbf{R}_{za,0}\mathbf{R}_{aa,0}^{-\frac{1}{2}}\right), \tag{16}$$

where covariance matrices are defined as $\mathbf{R}_{zz,0} = \mathbf{Z}_0\mathbf{Z}_0^{\mathrm{T}}$, $\mathbf{R}_{za,0} = \mathbf{Z}_0\mathbf{A}_{\mathrm{t},0}^{\mathrm{T}}$ and similarly for $\mathbf{R}_{aa,0}$ and $\mathbf{R}_{az,0}$. Notation $\mathrm{eig\,max}(\cdot)$ stands for the eigenvector associated to the maximum eigenvalue of the argument matrix. $\mathbf{R}_{aa,0}^{-1/2}$ is the inverse of the Cholesky factor of $\mathbf{R}_{aa,0}$: $\mathbf{R}_{aa,0} = \mathbf{R}_{aa,0}^{\mathrm{T}/2}\mathbf{R}_{aa,0}^{1/2}$. Solutions $\{\mathbf{w}_1, \hat{\mathbf{h}}_{w,11}\}$ for the other user ($i = 1$) are obtained from $\mathbf{Z}_1 = \mathbf{Y}_{\rm t} - \hat{\mathbf{H}}_0\mathbf{A}_{\mathrm{t},0}$ following the same approach as for user 0 on dual signals. The structure of the overall JOR system is shown in Fig. 3.

Intuitively, the filter application $\mathbf{w}_i^{\mathrm{T}}\mathbf{Y} = \mathbf{h}_{w,ii}^{\mathrm{T}}\mathbf{R}_{za,i}^{\mathrm{T}}\mathbf{R}_{zz,i}^{-\mathrm{T}}\mathbf{Y}$ is equivalent to a two-step processing: a whitening is first applied to the received signal $\mathbf{Y}$ using the inverse covariance matrix ($\mathbf{R}_{zz,i}^{-1}$) of the received signal after in-cell interference cancellation ($\mathbf{Z}_i$); the signal is then projected onto the subspace spanned by the dominant channel component selected by the eigenvalue decomposition (16). By such a decomposition the JOR identifies in the $(L+1)$-dimensional space the one-dimensional channel component that is associated with the maximum SINR value, which is the most relevant for data detection. This model follows the reduced rank (RR) approach described in [35]. It is essentially based on the assumption that the channel $\mathbf{H}_i$ can be approximated by a rank-1 matrix, i.e. $r_i = \mathrm{rank}(\mathbf{H}_i) \approx 1$. Low-rank channel matrices occur in propagation scenarios where the channel spread - in the spatial, temporal or I-Q domain - is lower than the maximum dimension allowed by the system. Under this condition, the channel rank is $r_i < r_{\max} = \min(4N_{\rm R}, L+1)$ and the channel can be parameterized by $2r_i$ hybrid ST and temporal filters. The one-dimensional JOR relies on the assumption that the number of filters is one, i.e. $\mathbf{H}_i \approx \mathbf{c}_i\mathbf{d}_i^{\mathrm{T}}$, where $\mathbf{c}_i$ is the $4N_{\rm R} \times 1$ hybrid ST component and $\mathbf{d}_i$ the $(L+1) \times 1$ temporal component. A more complete discussion about the relation between the RR estimation and the proposed approach is provided in Appendix VII-A.

In practical GSM scenarios, the maximum temporal support is determined by the training sequence length ($K_{\rm tsc} = 26$) and is $L \leq 12$. Practical receivers employ $L = 4$-5 which is suited for typical urban multipath environments (taking into account a delay spread of approximately 5μs and the GMSK pulse dispersion) [36] [37]. The number of receiving antennas is usually $N_{\rm R} = 2$, with large spacing for diversity. Under these conditions, it is $r_{\max} = 5$-6. The observed channel rank is typically determined by the spread in the hybrid ST domain as the degree of temporal diversity of the multipath channels is typically as large as the temporal support $L+1$. Taking into account the large antenna spacing and the GMSK pulse bandwidth, the hybrid ST rank is typically $r_i = 3$-6.

In practical scenarios, thereby, the true channel rank is usually higher than one. Still, reducing the rank by the JOR approach and tolerating some channel distortion might be beneficial for filtering out the inter-cell interference if the channel components that are discarded are associated to significantly low SINR values (i.e., the eigenvalues) compared to the dominant one. As shown by numerical results for practical GSM-OSC scenarios in Sec. VI, the GSM-OSC environment is fitting this assumption when the interfering scenario is highly correlated in the space-time domain, i.e. it is characterized by a small number of dominant interferers (e.g., one); in this case the beamforming by $\mathbf{w}_0$ allows to project the user signal into the space orthogonal to that of the dominant interference. If the number of the interferers increases, on the other hand, the interference tends to be white, the SINR over the channel components is not so unbalanced and a single beamformer

may be not sufficient. In this case, as described in Sec. IV, the bias introduced by the rank-1 approximation of $\mathbf{H}_0$ is too large and the JOR approach has to be modified into a multi-dimensional filtering where the number of space-time channel components is adaptively selected to maximize the system performance.

C. MUD Techniques for JOR

For joint detection of the two OSC users data from the filtered signals (10) we consider optimal non-linear JMLSE and suboptimal linear detection based on either Zero Forcing (ZF) or Minimum Mean Square Error (MMSE) criteria [24].

Let us rewrite the $2 \times (K_{\rm d}+L)$ signals (10) at the input of the detection stage as:

$$\mathbf{Y}_w = [\mathbf{y}_{w,0}, \mathbf{y}_{w,1}]^{\rm T} = \mathbf{H}_{w,0}\mathbf{A}_0 + \mathbf{H}_{w,1}\mathbf{A}_1 + \mathbf{N}_w, \quad (17)$$

where the $2 \times (L+1)$ matrices $\mathbf{H}_{w,0} = [\mathbf{h}_{w,00}, \mathbf{h}_{w,10}]^{\rm T}$ and $\mathbf{H}_{w,1} = [\mathbf{h}_{w,11}, \mathbf{h}_{w,01}]^{\rm T}$ gather the filtered channels while the residual interference is denoted as $\mathbf{N}_w = [\mathbf{n}_0, \mathbf{n}_1]^{\rm T}$.

Optimal detection requires a pre-whitening of the noise in (17) [24], using e.g. the LS estimate of the noise covariance obtained from the midamble as $\hat{\mathbf{R}}_n = \frac{1}{K_{\rm t}}\hat{\mathbf{N}}_{w,{\rm t}}\hat{\mathbf{N}}_{w,{\rm t}}^{\rm T}$, with $\hat{\mathbf{N}}_{w,{\rm t}} = \mathbf{Y}_{w,{\rm t}} - \hat{\mathbf{H}}_{w,0}\mathbf{A}_{{\rm t},0} - \hat{\mathbf{H}}_{w,1}\mathbf{A}_{{\rm t},1}$. The whitened signal is given by

$$\tilde{\mathbf{Y}}_w = \hat{\mathbf{R}}_n^{-\frac{\rm T}{2}}\mathbf{Y}_w = \tilde{\mathbf{H}}_{w,0}\mathbf{A}_0 + \tilde{\mathbf{H}}_{w,1}\mathbf{A}_1 + \tilde{\mathbf{N}}_w, \quad (18)$$

where $\tilde{\mathbf{H}}_{w,i} = \hat{\mathbf{R}}_n^{-{\rm T}/2}\mathbf{H}_{w,i}$ is the whitened channel matrix for the ith user. In the following, detection is performed over half a burst at a time ($K_{\rm d}$ data symbols), removing the response of the TSC and guard bits from the filtered signals.

1) Non-linear MUD: The joint maximum likelihood estimate of the two OSC users' data $\mathbf{a} = [a_0[1], ..., a_0[K_d], a_1[1], ..., a_1[K_d]]^{\rm T}$ is obtained as $\hat{\mathbf{a}} = \arg\min_{\mathbf{a}} J(\mathbf{a})$, by minimizing the negative log-likelihood function

$$J(\mathbf{a}) = \left\| \tilde{\mathbf{Y}}_w - \tilde{\mathbf{H}}_{w,0}\mathbf{A}_0 - \tilde{\mathbf{H}}_{w,1}\mathbf{A}_1 \right\|^2 \quad (19)$$

$$= \sum_{k=1}^{K_d+L} \underbrace{\left\| \tilde{\mathbf{y}}_w[k] - \tilde{\mathbf{H}}_{w,0}\mathbf{a}_0[k] - \tilde{\mathbf{H}}_{w,1}\mathbf{a}_1[k] \right\|^2}_{\Delta J_k(\mathbf{a}[k])}, \quad (20)$$

where $\tilde{\mathbf{y}}_w[k]$ denotes the kth column of $\tilde{\mathbf{Y}}_w$. The Viterbi algorithm [38] is used to exploit the recursive structure of the metric (19) and efficiently compute the two data sequence estimates over a trellis of 2^{2L} states and length $K_{\rm d}+L$ [25] [26], with branch metric $\Delta J_k(\mathbf{a}[k])$ depending on the bits $\mathbf{a}[k] = [\mathbf{a}_0^{\rm T}[k], \mathbf{a}_1^{\rm T}[k]]^{\rm T}$. The number of computations and memory requirements are linear in the number of states and thus increase exponentially with L. Soft outputs need to be provided to the channel decoder for ML decoding of the convolutional coded data[2]; to this aim, we evaluate the log-likelihood ratios (LLR) for all bits using the Soft Output Viterbi Algorithm (SOVA) approach [40].

[2]We recall that the coded stream is interleaved over a number of bursts experiencing different channel and interference conditions in order to provide fading diversity. Thereby for optimal channel decoding the equalizer must provide a soft estimate for all bits [39].

2) Linear MUD: Let us reorganize the whitened filtered signals of the semi-burst into the $2(K_{\rm d}+L) \times 1$ vector $\tilde{\mathbf{y}}_w = {\rm vec}(\tilde{\mathbf{Y}}_w^{\rm T}) = \tilde{\mathcal{H}}_w\mathbf{a} + \mathbf{n}_w$, where $\tilde{\mathcal{H}}_w$ is the $2(K_{\rm d}+L) \times 2K_{\rm d}$ convolution matrix for the filtered channels $\{\tilde{\mathbf{h}}_{w,00}, \tilde{\mathbf{h}}_{w,11}, \tilde{\mathbf{h}}_{w,01}, \tilde{\mathbf{h}}_{w,10}\}$ and $\mathbf{n}_w = [\mathbf{n}_0^{\rm T}, \mathbf{n}_1^{\rm T}]^{\rm T}$ is the overall residual noise plus interference. The ZF and MMSE solutions are given by, respectively, $\hat{\mathbf{a}}_s = (\tilde{\mathcal{H}}_w^{\rm T}\tilde{\mathcal{H}}_w)^{-1}\tilde{\mathcal{H}}_w^{\rm T}\tilde{\mathbf{y}}_w$ and $\hat{\mathbf{a}}_s = (\tilde{\mathcal{H}}_w^{\rm T}\tilde{\mathcal{H}}_w + \mathbf{I}_{2K_{\rm d}})^{-1}\tilde{\mathcal{H}}_w^{\rm T}\tilde{\mathbf{y}}_w$. Bit estimates are then obtained from $\hat{\mathbf{a}}_s$ using a threshold detector here denoted as $\hat{\mathbf{a}} = {\rm dec}(\hat{\mathbf{a}}_s)$. Each detected bit is associated with a LLR value for soft decoding of the convolutionally coded data using a Gaussian model for the BPSK data estimate as in [41], with variance $\hat{\sigma}_n^2 = \frac{1}{2K_{\rm d}}||\hat{\mathbf{a}}_s - \hat{\mathbf{a}}||^2$.

IV. Multi-dimensional JOR-r

The approach in Sec. III relies on the assumption that the user channel, usually full rank, can be approximated by a dominant rank-1 component characterized by a SINR value significantly higher than those discarded and associated with the other channel components. When this is not the case, as in rich spatial-temporal dispersive channels with spatially distributed interference, all signal dimensions experience comparable SINR conditions and the receiver performance has to be improved by selecting multiple channel components, as shown later in Sec. VI for realistic GSM-OSC scenarios. In this section we introduce the multiple component JOR (JOR-r) obtained by modifying the JOR structure with the use of $r \geq 1$ filters per OSC user in the beamforming stage and adapting the MUD stage to the new multi-dimensional filtered signals (see Fig. 4). Filters' derivation is obtained by extending the RR approach discussed in Section III-B to a rank-r estimation for each user. The optimal detection architecture is a cascade of a set of r hybrid ST filters for each user, followed by a multi-user MLSE detection with branch metric depending on the $2r$ temporal filters for the two OSC users (see also [46] for multipath space-time CDMA systems); we refer to this structure as JOR-JMLSE. The drawback is the higher receiver complexity, as the dimensions of the signals to be processed by MUD increases with the number of filters. A lower complexity receiver is provided by linear detection, leading to the JOR-LMUD structure. For both linear and non-linear detection, the number of filters r should be selected as trade-off between the receiver performance and its computational complexity depending on the channel/interference conditions. Practically, this choice can be carried out by means of numerical simulations of the reference environment. Notice also that the number r that maximizes the receiver performance might be lower than the true channel rank, as the optimal value for r is the one that yields the best compromise between channel estimate bias and interference reduction [35], as proved later by simulation results.

A. Multiple Filter Derivation

We consider a set of $r \leq r_{\max}$ filters, stacked in the $4N_{\rm R} \times r$ matrix $\mathbf{W}_i = [\mathbf{w}_i^{(1)}, ..., \mathbf{w}_i^{(r)}]$, for each user i. The two $r \times (K+L)$ matrices gathering the filtered signals for the two

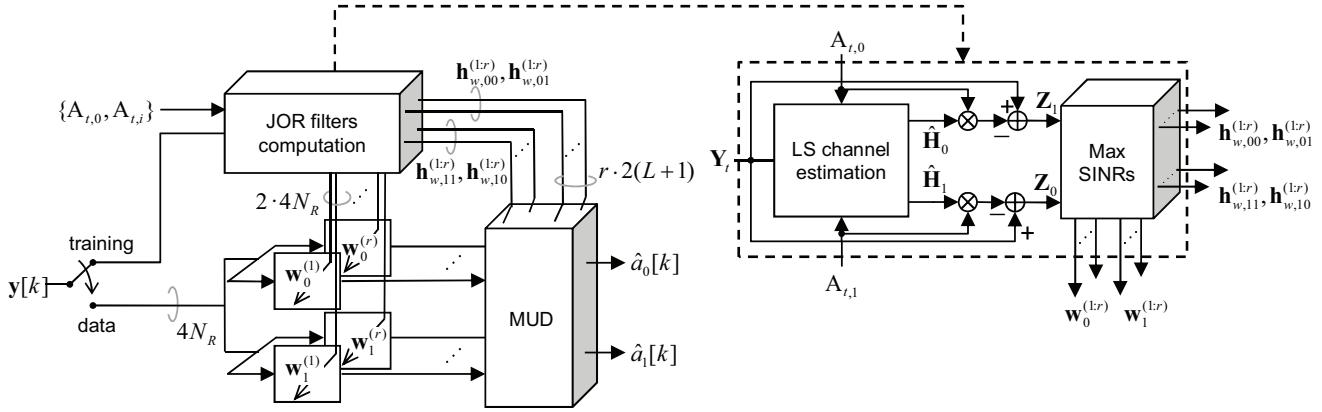

Fig. 4. Multi-dimensional JOR structure: r filters are applyed to the received signal for each OSC user. The filtered signals and channel responses are combined in the MUD block.

OSC users, $i = 0$ and $i = 1$, are denoted as:

$$\begin{cases} \mathbf{Y}_{w,0}^{\mathrm{T}} = \mathbf{W}_0^{\mathrm{T}}\mathbf{Y} = \mathbf{H}_{w,00}^{\mathrm{T}}\mathbf{A}_0 + \mathbf{H}_{w,01}^{\mathrm{T}}\mathbf{A}_1 + \mathbf{N}_0^{\mathrm{T}} \\ \mathbf{Y}_{w,1}^{\mathrm{T}} = \mathbf{W}_1^{\mathrm{T}}\mathbf{Y} = \mathbf{H}_{w,10}^{\mathrm{T}}\mathbf{A}_0 + \mathbf{H}_{w,11}^{\mathrm{T}}\mathbf{A}_1 + \mathbf{N}_1^{\mathrm{T}} \end{cases} \quad (21)$$

where the $(L+1)\times r$ matrix $\mathbf{H}_{w,ii} = [\mathbf{h}_{w,ii}^{(1)}, ..., \mathbf{h}_{w,ii}^{(r)}]$ collects the r filtered channel responses for user i, $\mathbf{H}_{w,01}^{\mathrm{T}} = \mathbf{W}_0^{\mathrm{T}}\mathbf{H}_{w,1}$ and $\mathbf{H}_{w,10}^{\mathrm{T}} = \mathbf{W}_1^{\mathrm{T}}\mathbf{H}_{w,0}$ are the cross-channels and $\mathbf{N}_i$ is the filtered noise. Filter derivation is carried out as in Sec. III-B by maximizing the SINR of the ith user with respect to the r ST filters $\mathbf{W}_i$ and the corresponding r temporal channel responses $\mathbf{H}_{w,i}$:

$$\left\{\mathbf{W}_i, \hat{\mathbf{H}}_{w,ii}\right\} = \underset{\mathbf{W}_i, \mathbf{H}_{w,ii}}{\arg\max} \ \mathrm{SINR}_i. \quad (22)$$

For $i = 0$ (and similarly for $i = 1$), the SINR is defined as:

$$\mathrm{SINR}_0 = \frac{\left\|\mathbf{H}_{w,00}^{\mathrm{T}}\mathbf{A}_{\mathrm{t},0}\right\|^2}{\left\|\mathbf{W}_0^{\mathrm{T}}\mathbf{Y}_{\mathrm{t}} - \mathbf{W}_0^{\mathrm{T}}\hat{\mathbf{H}}_1\mathbf{A}_{\mathrm{t},1} - \mathbf{H}_{w,00}\mathbf{A}_{\mathrm{t},0}\right\|^2} \quad (23)$$

$$= \frac{\left\|\mathbf{H}_{w,00}^{\mathrm{T}}\mathbf{A}_{\mathrm{t},0}\right\|^2}{\left\|\mathbf{W}_0^{\mathrm{T}}\mathbf{Z}_0 - \mathbf{H}_{w,00}\mathbf{A}_{\mathrm{t},0}\right\|^2}, \quad (24)$$

where $\mathbf{Z}_0 = \mathbf{Y}_{\mathrm{t}} - \hat{\mathbf{H}}_1\mathbf{A}_{\mathrm{t},1}$. The optimization leads to the solution (see Appendix A):

$$\mathbf{W}_0 = \mathbf{R}_{zz,0}^{-1}\mathbf{R}_{za,0}\hat{\mathbf{H}}_{w,00} \quad (25)$$

$$\hat{\mathbf{H}}_{w,00} = \mathbf{R}_{aa,0}^{-\frac{1}{2}}\underset{r}{\mathrm{eig\,max}}\left(\mathbf{R}_{aa,0}^{-\frac{\mathrm{T}}{2}}\mathbf{R}_{az,0}\mathbf{R}_{zz,0}^{-1}\mathbf{R}_{za,0}\mathbf{R}_{aa,0}^{-\frac{1}{2}}\right), \quad (26)$$

where $\mathrm{eig\,max}_r(\cdot)$ indicates the set of the r leading eigenvectors of the argument matrix. The $2r \times (K_{\mathrm{d}} + L)$ filtered signal can be expressed as:

$$\mathbf{Y}_w = [\mathbf{Y}_{w,0}, \mathbf{Y}_{w,1}]^{\mathrm{T}} = \mathbf{H}_{w,0}\mathbf{A}_0 + \mathbf{H}_{w,1}\mathbf{A}_1 + \mathbf{N}_w, \quad (27)$$

where the $2r \times (L + 1)$ matrices $\mathbf{H}_{w,0} = [\mathbf{H}_{w,00}, \mathbf{H}_{w,10}]^{\mathrm{T}}$, $\mathbf{H}_{w,1} = [\mathbf{H}_{w,11}, \mathbf{H}_{w,01}]^{\mathrm{T}}$ represent the filtered channels and $\mathbf{N}_w = [\mathbf{N}_0, \mathbf{N}_1]^{\mathrm{T}}$ the residual interference.

B. Multi-dimensional MUD

The filtered signal (27) is processed by the (either linear or non-linear) multi-user detectors described in Sec. III-C,

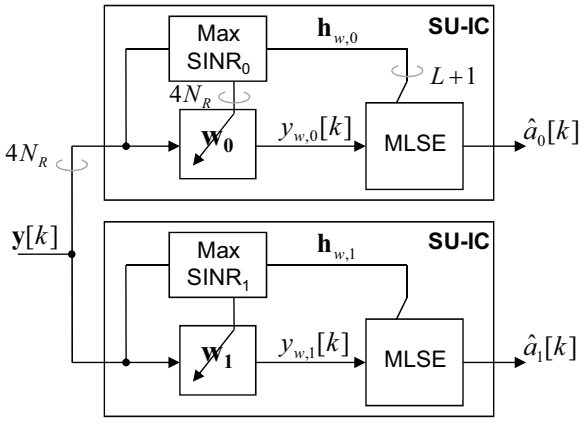

Fig. 5. SU-IC receiver structure. A prefilter is applyed to the received signal maximizing the SINR of a single OSC channel.

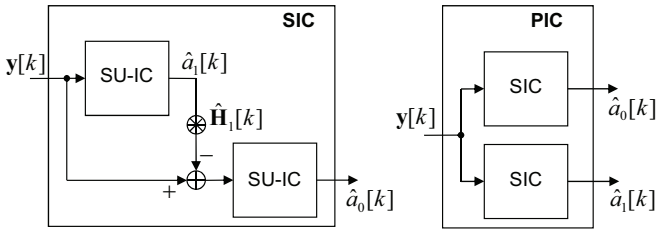

Fig. 6. SIC and PIC receiver structures.

with matrices and vectors redefined according to the multi-dimensional filtering case.

Pre-whitening of the filtered signal is performed using the $2r \times 2r$ noise covariance estimate $\hat{\mathbf{R}}_n = \frac{1}{K_{\mathrm{t}}}\hat{\mathbf{N}}_{w,\mathrm{t}}\hat{\mathbf{N}}_{w,\mathrm{t}}^{\mathrm{T}}$ relative to the signal model (27). The resulting $2r \times (K_{\mathrm{d}} + L)$ whitened signal is $\tilde{\mathbf{Y}}_w = [\tilde{\mathbf{Y}}_{w,0}, \tilde{\mathbf{Y}}_{w,1}]^{\mathrm{T}} = \hat{\mathbf{R}}_n^{-\mathrm{T}/2}\mathbf{Y}_w$, while $\tilde{\mathbf{H}}_{w,i} = \hat{\mathbf{R}}_n^{-\mathrm{T}/2}\mathbf{H}_{w,i}$ is the $2r \times (L + 1)$ corresponding whitened channel response.

For optimal non-linear MUD, the Viterbi algorithm is implemented using the above defined signals $\tilde{\mathbf{Y}}_w$ and $\tilde{\mathbf{H}}_{w,i}$ for the JMLSE metric computation (19). On the other hand, the linear MUD schemes are applied to the $2r(K + L) \times 1$ vectorized signal $\tilde{\mathbf{y}}_w = \mathrm{vec}(\tilde{\mathbf{Y}}_w^{\mathrm{T}})$ using the $2r(K + L) \times 2K$ convolution channel matrix $\tilde{\mathcal{H}}_w$.

V. Overview of Existing Receivers

In this section we recall some well known interference mitigation techniques, here adapted to the uplink of the GSM-OSC scenario, to be used as benchmarks for JOR evaluation in Sec. VI:

- *Single-User Maximum Ratio Combining (SU-MRC)* is the optimal combiner of the signals at different antennas for detection of a single user stream in a scenario where the second OSC channel has been disabled. This case of no in-cell interference[3] will be considered as reference for performance assessment of the JOR algorithm. The signal (1) is sampled over each antenna at the symbol rate $\bar{\mathbf{y}}[k] = \bar{\mathbf{y}}(kT)$. Let the $N_{\mathrm{R}} \times 1$ vector $\widehat{\bar{\mathbf{h}}}_0[k]$, with $k = 0, ..., L$, denote the LS estimate of the user channel response at the symbol rate, the SU-MRC receiver uses this estimate to optimally combine the multi-antenna signals [42]:

$$y_{\mathrm{MRC}}[k] = \sum_{\ell=1}^{L} \widehat{\bar{\mathbf{h}}}_0^{\mathrm{H}}[k-\ell]\ \bar{\mathbf{y}}[k]. \tag{28}$$

  The filtered signal is then used in a MLSE equalizer [38] to recover the transmitted sequence $\{a_0[k]\}$ employing a SOVA with 2^L states [40].
- *Joint Maximum Likelihood Sequence Estimation* (*JMLSE)* of the OSC streams $\{a_0[k], a_1[k]\}$ is obtained through a multi-antenna JMLSE equalizer (without any prefiltering stage for out-of-cell interference). It can be implemented by a SOVA with 2^{2L} states applied to the complex received signals (1) sampled at baud-rate (see [26] for details). Signals at the N_{R} antennas are optimally combined in the branch metric of the SOVA trellis.
- *Single-User Interference Cancellation (SU-IC)* detects one OSC user at a time (see Fig. 5) using conventional interference filtering technologies developed for the DARP phase I-II receivers [4] such as SAIC for $N_{\mathrm{R}} = 1$ or DAIC for $N_{\mathrm{R}} = 2$ or MAIC extensions for higher number of antennas [22]. It should be noted that no standardized versions of these receivers are available, only different vendors solutions. Here, for each ith OSC user, a prefilter $\mathbf{w}_i$ is designed so as to maximize the SINR with respect to the overall interference, i.e. the out-of-cell interference *and* the impairment from the other OSC user:

$$\mathrm{SINR}_i = \frac{\|\mathbf{h}_{w,i}\mathbf{A}_{\mathrm{t},i}\|^2}{\left\|\mathbf{w}_i^{\mathrm{T}}\mathbf{Y}_{\mathrm{t}} - \mathbf{h}_{w,ii}\mathbf{A}_{\mathrm{t},i}\right\|^2}, \tag{29}$$

  obtaining the filter $\mathbf{w}_i$ and the relative filtered channel $\mathbf{h}_{w,ii}$. Notice that, differently from JOR, the two filters are designed independently for the two users. The received signals are then filtered by $\{\mathbf{w}_1, \mathbf{w}_2\}$ and the two streams are separately processed by two MLSE equalizers using the channel responses $\{\mathbf{h}_{w,11}, \mathbf{h}_{w,22}\}$ (Fig. 5).
- *Successive Interference Cancellation (SIC)* is a two-stage approach that, as sketched in Fig. 6 (left sub-figure), detects at first the strongest OSC user sequence from the received signal, then it re-modulates and subtracts the detected sequence from the received signal to allow the detection of the other OSC user sequence [11]. For the detection of each stream here we use the SU-IC algorithm.
- *Parallel Interference Cancellation (PIC)* is implemented by two parallel SIC receivers applied separately to obtain $a_0[k]$ and $a_1[k]$, as described in Fig. 6 (right sub-figure). PIC requires to employ the SU-IC four times with a filter calculation and a MLSE equalizer each.

[3]MRC cannot cope with the fully interfered OSC transmission [11]

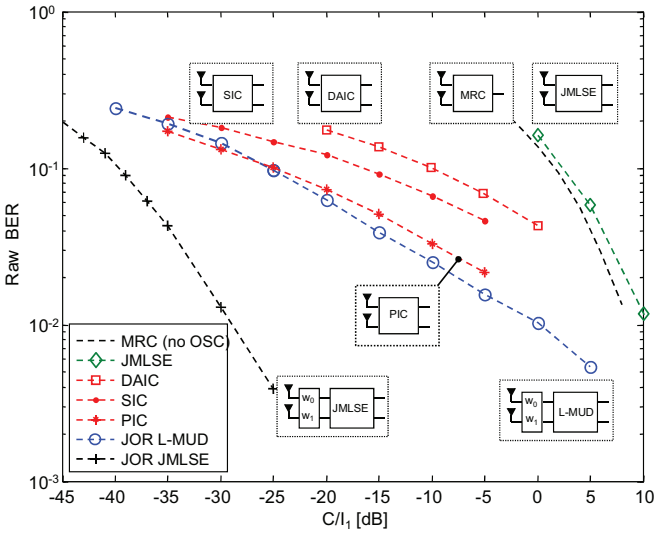

Fig. 7. BER vs $\mathrm{C/I}_1$ for JOR-1 and other receiving schemes in the MUROS MTS-1 scenario.

VI. Numerical Results

The performances of the receivers described in previous sections are here evaluated through Montecarlo simulation of a standard-compliant GSM-OSC cellular environment at 900MHz. In the cell of interest, a BS equipped with $N_{\mathrm{R}} = 2$ antennas receives the signals generated by two in-cell OSC users and V out-of-cell interferers. All MSs move at 3km/h. The two OSC users transmit GMSK modulated data bursts including, respectively, a GSM conventional TSC and a new TSC as specified in the OSC feature proposal [11]. According to the assumption of ideal frequency hopping (i.e., block fading) and receive spatial diversity, independent realizations of channels are generated for each burst, user and receiving antenna. The multipath channel is simulated according to the Typical Urban (TU) COST-207 channel model [10]. The receiver assumes a channel length of $(L + 1) = 5$ time symbols. The front-end receive filter has a raised root cosine impulse response with roll-off $\alpha = 0.3$ and 3dB bandwidth 240kHz. All interferers are designed as MSs transmitting GMSK streams. This approach includes both the case of traditional users and of VAMOS aware MSs. As a matter of fact when adopting the OSC technique, each MS is still transmitting a GMSK signal but employing a TSC selected from a wider set. Here the interferers use random binary sequences as TSCs as the bursts are supposed to be not synchronized between neighboring cells.

The average performances of the generic OSC user are assessed by considering the Bit Error Rate at the output of the MUD process (raw BER) and the Frame Error Rate (FER)

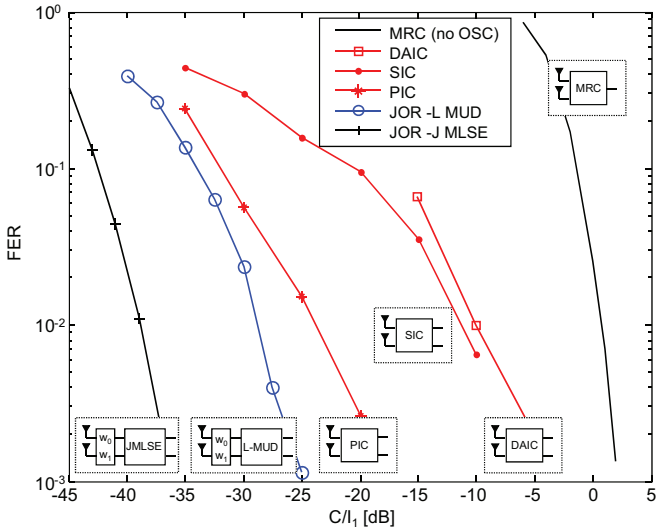

Fig. 8. FER vs C/I_1 for JOR-1 and other receiving schemes in the MUROS MTS-1 scenario.

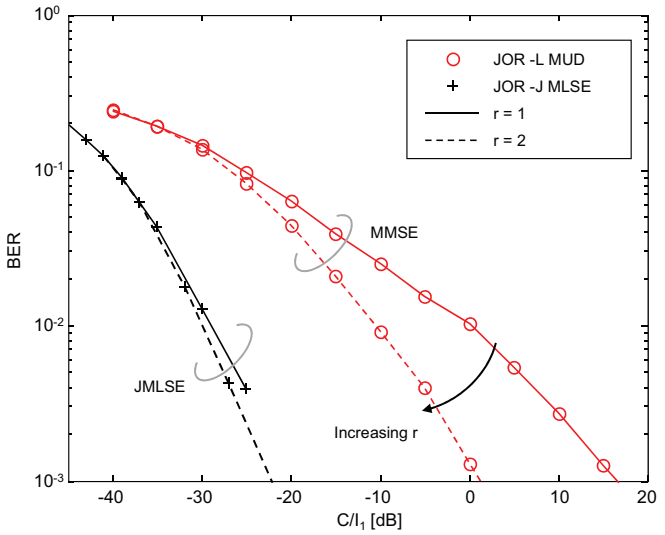

Fig. 10. BER vs C/I_1 for JOR-r with $r = \{1, 2\}$ pre-filters per OSC user, and either JMLSE or MMSE linear detection, in the MUROS MTS-1 scenario.

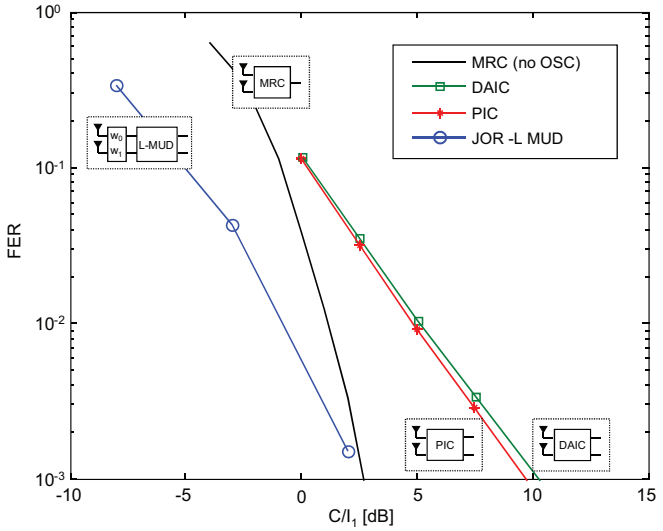

Fig. 9. FER vs C/I_1 for JOR-1 and other receiving schemes in the MUROS MTS-2 scenario.

for an Adaptive Full Speech (AFS) coded transmission with 5.9 kbit/s as specified in [9]. The performance curves are drawn as a function of the carrier-to-interference ratio (C/I) defined as $C/I_1 = P_0/P_{I,1}$ where $P_0 = E[\|\bar{\mathbf{h}}_0(k)\|^2] = P_1$ is the average receive power of each OSC user (perfect power control is assumed), while $P_{I,1}$ is the average receive power for the dominant interferer. The signal to noise ratio is defined as $SNR = P_0/\sigma^2_{bn}$ where σ^2_{bn} is the background noise power. Different multi-cell environments are simulated according to the MUROS Test Scenarios (MTSs) described in [43].

Fig. 7 and 8 compare the performances of the JOR-1 solution and the other considered receiving schemes in terms of raw BER and FER. The interference-limited MUROS scenario MTS-1 has been simulated, with a single out-of-cell interferer (i.e., $V = 1$) and no background noise. It can be noted that the JMLSE equalizer without any prefiltering stage experiences the worst performance. In fact, JMLSE is the optimum receiver in case of AWGN but it cannot cope with correlated interference (e.g., in the OSC scenario) where the prefilter becomes mandatory. Also the performance of the single-user MRC is unsatisfactory, as this receiver does not account for the interfering OSC user signal. Notice that neither single-user MRC nor JMLSE exploits the non-circularity of OSC signals for interference mitigation, so the performance degradation is considerable. On the other hand, both SIC and PIC approaches offer reasonable performance (with moderate computational complexity). The JOR-1 filter has been implemented using both the JMLSE and the linear MMSE (L-MUD) schemes for the MUD stage. As expected, the optimal non-linear detection outperforms all the other solutions, but its 256 states can be a strong limitation for hardware implementation. A better trade-off between computational cost and performance is reached by the linear MUD that guarantees good performance with a reasonable computational complexity.

A more challenging interference-limited environment is analyzed in Fig. 9 according to the MUROS MTS-2 testing scenario. Two out-of-cell interferers are simulated with power ratio $P_{I,1}/P_{I,2} = 10$dB on the same subcarrier used for the OSC users $i = 0$ and $i = 1$; an intra-cell interferer occupying an adjacent subcarrier is transmitting with $P_0/P_{I,3} = 3$dB (power is evaluated at the input of the receiving filter); AWGN is simulated with $SNR = -17$dB. Fig. 9 reports the FER curves vs C/I_1 for DAIC, PIC and JOR (with linear MMSE detection). It should be noted that all the performance curves are subject to a huge shift along the C/I_1 axis if compared to the MTS-1 case (see Fig. 8). The presence of 3 interferers plus a strong background noise causes a severe degradation of the prefiltering performance. Differently from the MTS-1 scenario, here the interference is stronger over all channel bases. Even in such a complex scenario, the JOR receiver selecting the channel component with the highest SINR is able to provide a gain of approximately 7-8dB w.r.t. conventional DAIC and PIC approaches.

As observed in Section IV, in practical GSM scenarios the channel rank is usually higher than one. The optimal receiver for such scenarios is the JOR-r, with r prefilters

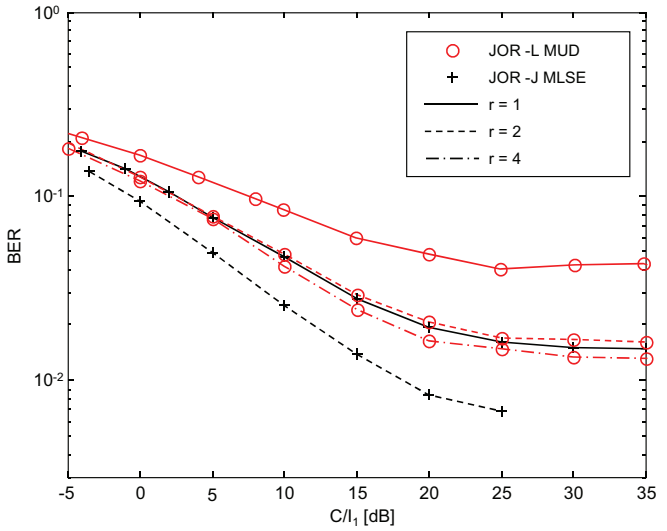

Fig. 11. BER vs C/I_1 for JOR-r with $r = \{1, 2, 4\}$ pre-filters per OSC user and either JMLSE or MMSE linear detection, in the MUROS MTS-2 scenario.

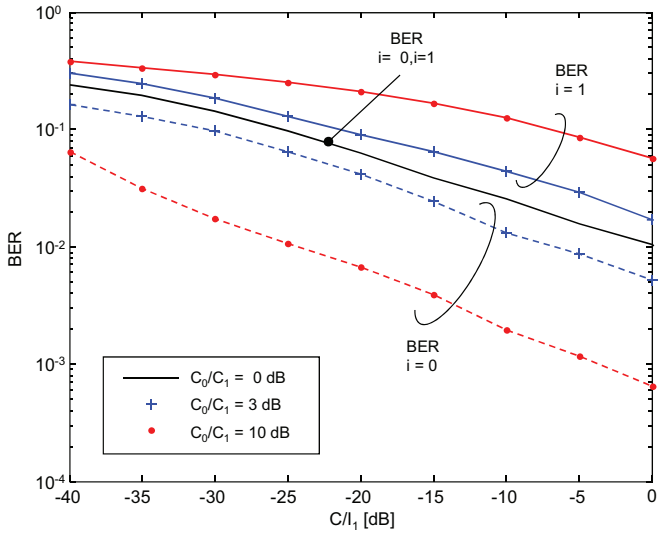

Fig. 12. Near-far BER performance for user $i = 0$ in the MUROS MTS-1 scenario with JOR-1 receiver and MMSE linear detection.

for each user, followed by a multi-user JMLSE. The order r to be used in the JOR-r structure might be lower than the true channel rank, as the optimal value is the one that provides the best distortion/variance tradeoff. This is shown in Fig. 10 and Fig. 11 where the multi-dimensional JOR-r performance with $r = \{1, 2\}$ is evaluated in terms of BER vs C/I_1, for the MTS-1 and MTS-2 scenarios, respectively. Both JMLSE and MMSE linear detection are considered for the MUD stage. In the MTS-1 case, the use of $r = 2$ filters with linear detection provides a significant gain over the one-dimensional JOR (about 10dB at 1% of BER), while for JMLSE multiple filters do not introduce significant gain. In the MTS-2 environment the performances are subject to a general shift over the C/I_1 axis and the curves reach a floor due to the constant background noise and adjacent-channel interferer. Considering Fig. 11 at 10% of BER, it can be observed that JOR-2 provides a gain of 4dB with respect to JOR-1 in case of linear detection and 2dB for the non-linear approach. For the L-MUD case, in particular, increasing the number of filters from $r = 2$ to $r = 4$ does not introduce a noticeable improvement. Since every additional dimension included in the receiver increases significantly the computational complexity, a trade-off between performance and computational complexity is mandatory. For the scenario here considered we can conclude that the best trade-off is obtained for $r = 2$; it is not worth to further increase the number of dimensions.

Fig. 12 shows the performance degradation in case of unbalanced user powers (i.e., near-far effect). Here the JOR prefilter has been coupled with MMSE L-MUD. The figure draws the raw BER performances for different power-ratios between the OSC users: $P_0/P_1 = \{0, 3, 10\}$dB. In case of equal power allocation ($P_0/P_1 = 0$dB), the performance of both users are identical since their SINRs are comparable (black curve without markers in the figure). When the power ratio increases, the BER of user $i = 0$ decreases due to the reduction of the in-cell interference while user $i = 1$ suffers for poorer performance. It is clear that we obtain the opposite result if we consider $P_0/P_1 = \{-3, -10\}$dB. As expected, numerical results show that, for the UL scenario, the best strategy is to maintain the power received from the OSC users as much comparable as possible to guarantee a fair detection of both users. This needs to be considered by resource allocation strategies for user pairing.

Finally, Fig. 13 analyzes the BER performance of the OSC transmission in a sensitivity scenario where only the background noise has been simulated. In realistic working conditions this scenario is less likely to be found since the frequency reuse of the cellular environment does introduce co-cell interference. However the sensitivity case gives information about how increasing background noise can affect the receiving performance. JOR with $r = 1$ and non-linear MUD is the solution that can handle the noise at best, while we have to account for more than one filter ($r = 2$) to reach the same BER with the linear approach. These two JOR setups provide comparable performance with all the other receivers.

VII. Conclusions

The pushing demand for voice traffic made the 3GPP group to investigate new solutions to increase the system capacity of the GSM/EDGE existing networks. The OSC multiplexing scheme is one of the latest standardized techniques that allows to double the number of served GSM devices by a simple re-configuration of the existing hardware. In this paper we focused on the UL scenario of a GSM-OSC system and we proposed a novel receiver specifically derived for the new environment. The structure of the JOR scheme relies on a two stage processing: a set of prefilters optimized to maximize the SINR of the two OSC users with respect to the out-of-cell interference and a MUD designed to jointly recover the two transmitted sequences. The JOR scheme has been designed with a variable number of filters so as to adapt to heterogeneous multi-cell propagation scenarios. Numerical results show that the proposed algorithm outperforms existing receivers, providing a gain from 3dB to 7dB depending

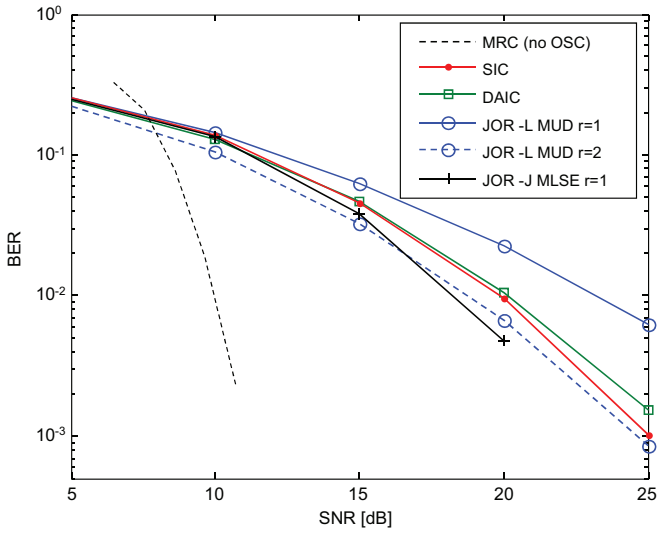

Fig. 13. BER vs SNR for JOR-r and other receiving schemes in a sensitivity (interference-free) scenario.

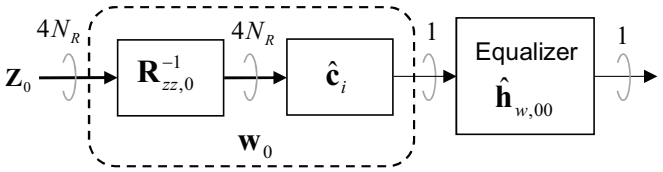

Fig. 14. Reduced rank receiver structure.

on the selected multicell scenario. Furthermore the multi-dimensional approach allows to improve performance while meeting service requirements and complexity constraints.

ACKNOWLEDGMENT

The authors would like to thank the former student M. Minelli for his contribution to the development of the GSM-OSC simulation environment, U. Spagnolini for helpful discussions, C. Masseroni and S. Parolari from Nokia Siemens Networks for their guidelines on the definition of practical GSM-OSC scenarios.

APPENDIX

A. JOR and Reduced Rank (RR) filtering approach

In the following, the JOR architecture, as derived in Sec. III-B, is described adopting the RR channel model [35]. The RR approach eases to figure out the processing steps providing a better understanding of the filtering architecture. The JOR filters (15)-(16) can be seen as the filters matched to the rank-1 estimate of the channel matrix $\mathbf{H}_i$ obtained from signal $\mathbf{Z}_i$ under the rank-1 constraint $\mathbf{H}_i \approx \mathbf{c}_i\mathbf{d}_i^{\mathrm{T}}$, where $\mathbf{c}_i$ is the $4N_{\mathrm{R}} \times 1$ hybrid ST component and $\mathbf{d}_i$ the $(L+1)\times 1$ temporal component of the channel.

The single-user rank-1 maximum likelihood estimate[4] for user i from signal $\mathbf{Z}_i$ is indeed $\widehat{\mathbf{H}}_i = \hat{\mathbf{c}}_i\hat{\mathbf{d}}_i^{\mathrm{T}}$ with [35]:

$$\hat{\mathbf{c}}_i = \mathbf{R}_{za,i}\mathbf{R}_{aa,i}^{-\frac{1}{2}}\mathbf{u}_i \quad (30)$$

$$\hat{\mathbf{d}}_i = \mathbf{R}_{aa,i}^{-\frac{1}{2}}\mathbf{u}_i \quad (31)$$

[4]Under the Gaussian assumption for the noise and the interference.

where $\mathbf{u}_i = \mathrm{eig}\max\left(\widehat{\tilde{\mathbf{H}}}_i^{\mathrm{T}}\widehat{\tilde{\mathbf{H}}}_i\right)$ is the dominant eigenvector of the (whitened) estimated channel $\widehat{\tilde{\mathbf{H}}}_i = \mathbf{R}_{zz,i}^{-1/2}\mathbf{R}_{za,i}\mathbf{R}_{aa,i}^{-1/2}$.

The single-user optimal receiver for such a rank-1 channel is the cascade of a whitened matched filter - matched to the hybrid ST component estimate $\hat{\mathbf{c}}_i$ - followed by an equalizer for the temporal component estimate $\hat{\mathbf{d}}_i$. The whitening matched filter equals the JOR pre-filter $\mathbf{w}_i = \mathbf{R}_{zz,i}^{-1}\hat{\mathbf{c}}_i$, while the temporal component equals the JOR temporal filter $\hat{\mathbf{d}}_i = \hat{\mathbf{h}}_{w,ii}$. The receiver designed for the single rank channel is sketched in Fig. 14 for $i = 0$.

It should be noticed that, differently from a conventional single-user rank-1 receiver, in the proposed JOR architecture the whitened matched filter is applied to the multi-user signal $\mathbf{Y}$ (not the signal $\mathbf{Z}_i$ which is used only to derive the filters' coefficients and it is defined within the training stream where we have knowledge of the co-user data). Hence, equalization must be performed jointly for the two OSC users to remove the residual mutual interference, through the MUD stage.

B. Multi-dimensional JOR Filter Derivation

For user $i = 0$, the denominator of the SINR (23) can be conveniently rewritten as:

$$\left\|\mathbf{W}_0^{\mathrm{T}}\mathbf{Z}_0 - \mathbf{H}_{w,00}^{\mathrm{T}}\mathbf{A}_{\mathrm{t},0}\right\|^2 = \mathrm{tr}\left[\mathbf{H}_{w,00}^{\mathrm{T}}\mathbf{B}\mathbf{H}_{w,00}\right] + \mathrm{tr}\left[\mathbf{F}^{\mathrm{T}}\mathbf{R}_{zz,0}^{-1}\mathbf{F}\right]$$

with $\mathbf{B} = \mathbf{R}_{aa,0} - \mathbf{R}_{az,0}\mathbf{R}_{zz,0}^{-1}\mathbf{R}_{za,0}$ and $\mathbf{F}=\mathbf{R}_{zz,0}\mathbf{W}_0 - \mathbf{R}_{za,0}\mathbf{H}_{w,00}$. Therefore the SIR becomes:

$$\mathrm{SINR}_0 = \frac{\mathrm{tr}\left[\mathbf{H}_{w,00}^{\mathrm{T}}\mathbf{R}_{aa,0}\mathbf{H}_{w,00}\right]}{\mathrm{tr}\left[\mathbf{H}_{w,00}^{\mathrm{T}}\mathbf{B}\mathbf{H}_{w,00}\right] + \mathrm{tr}\left[\mathbf{F}^{\mathrm{T}}\mathbf{R}_{zz,0}^{-1}\mathbf{F}\right]} \quad (32)$$

where $\mathrm{tr}\left[\mathbf{F}^{\mathrm{T}}\mathbf{R}_{zz,0}^{-1}\mathbf{F}\right] \geq 0$. The quotient is maximized when this last term is zero, that is for $\mathbf{F} = \mathbf{0}$, which leads to (25). By substituting this result into (32), we get:

$$\mathrm{SINR}_0 = \frac{\mathrm{tr}\left[\mathbf{H}_{w,00}^{\mathrm{T}}\mathbf{R}_{aa,0}\mathbf{H}_{w,00}\right]}{\mathrm{tr}\left[\mathbf{H}_{w,00}^{\mathrm{T}}\left(\mathbf{R}_{aa,0} - \mathbf{R}_{az,0}\mathbf{R}_{zz,0}^{-1}\mathbf{R}_{za,0}\right)\mathbf{H}_{w,00}\right]}. \quad (33)$$

The maximization of the above expression is an extended Rayleigh quotient problem [44] (or multidimensional Rayleigh quotient [45]) whose solution is:

$$\mathbf{R}_{aa,0}^{\frac{1}{2}}\hat{\mathbf{H}}_{w,00} = \mathrm{eig}\min_r\left(\mathbf{I}_{L+1} - \mathbf{R}_{aa,0}^{-\frac{\mathrm{T}}{2}}\mathbf{R}_{az,0}\mathbf{R}_{zz,0}^{-1}\mathbf{R}_{za,0}\mathbf{R}_{aa,0}^{-\frac{1}{2}}\right)$$
$$= \mathrm{eig}\max_r\left(\mathbf{R}_{aa,0}^{-\frac{\mathrm{T}}{2}}\mathbf{R}_{az,0}\mathbf{R}_{zz,0}^{-1}\mathbf{R}_{za,0}\mathbf{R}_{aa,0}^{-\frac{1}{2}}\right). \quad (34)$$

The above result proves (26).

REFERENCES

[1] Informa Telecoms & Media, WCIS+, Sept. 2010, www.4gamericas.org.
[2] Nokia Siemens Networks, "Doubling GSM voice capacity with the orthogonal Sub channel," technology brief, http://www.nsn.com.
[3] 3GPP TS 45.015 v9.0, "Release independent downlink advanced receiver performance (DARP): implementation guidelines," 3GPP GERAN, Dec. 2009.
[4] P. A. Hoeher, S. Badri-Hoeher, W. Xu, and C. Krakowski, "Single-antenna co-channel interference cancellation for TDMA cellular radio systems," *IEEE Wireless Commun.*, vol. 12, no. 2, pp. 30–37, Apr. 2005.
[5] P. A. Hoeher, S. Badri-Hoeher, S. Deng, C. Krakowski, and W. Xu, "Single antenna interference cancellation (SAIC) for cellular TDMA networks by means of joint delayed-decision feedback sequence estimation," *IEEE Trans. Wireless Commun.*, vol. 5, pp. 1234–1237, June 2006.

[6] 3GPP TR 45.914 v8.2.0 "Circuit Switched Voice Capacity Evolution for GSM/EDGE Radio Access Network (GERAN)," 3GPP GERAN, Sept. 2009.
[7] R. Meyer, W. H. Gerstacker, R. Schober, and J. B. Huber, "A single antenna interference cancellation algorithm for increased GSM capacity," *IEEE Trans. Wireless Commun.*, vol. 5, no. 7, pp. 1616–1621, July 2006.
[8] P. Chevalier and P. F. Pipon, "New insights into optimal widely linear array receivers for the demodulation of BPSK, MSK, and GMSK signlas corrupted by noncircular interferences—application to SAIC," *IEEE Trans. Signal Process.*, vol. 54, no. 3, pp. 870–883, Mar. 2006.
[9] 3GPP TS 45.004 v9.1, "Modulation," 3GPP GERAN, June 2010.
[10] M. Säily, G. Sébire, and E. Riddington, *GSM/EDGE: Evolution and Performance*, 1st edition. Wiley, 2010.
[11] GP-071792, "Voice capacity evolution with orthogonal sub channels," Nokia Siemens Networks, 3GPP GERAN#36, Vancouver, Canada, Nov. 2007.
[12] X. Chen, Z. Fei, J. Kuang, L. Liu, and G. Yang, "A scheme of multi-user reusing one slot on enhancing capacity of GSM/EDGE networks," in *Proc. 2008 IEEE Singapore Int. Conf. on Commun. Syst.*, pp. 1574–1578.
[13] D. Molteni, M. Nicoli, and U. Spagnolin, "Performance of MIMO-OFDMA systems in correlated fading channels and non-stationary interference," *IEEE Trans. Wireless Commun.*, vol. 10, no. 5, pp. 1480–1494, May 2011.
[14] J. W. Liang, J. T. Chen, and A. J. Paulraj, "A two-stage hybrid approach for CCI/ISI reduction with space-time processing," *IEEE Commun. Lett.*, vol. 1, pp. 163–165, Nov. 1997.
[15] Y. K. Lee, R. Chandrasekaran, and J. J. Shynk, "Separation of cochannel GSM signals using an adaptive array," *IEEE Trans. Signal Process.*, vol. 47, no. 7, July 1999.
[16] U. Spagnolini, "Adaptive rank-one receiver for GSM/DCS systems," *IEEE Trans. Veh. Technol.*, vol. 51, no. 5, pp. 1264–1271, Sept. 2002.
[17] M. Vutukuri, R. Malladi, K. Kuchi, and R. Koilpillai, "SAIC receiver algorithms for VAMOS downlink transmission," in *Proc. 2011 International Symposium on Wireless Communication Systems*, pp. 31–35.
[18] P. Chevalier and F. Dupuy, "Widely linear Alamouti receiver for the reception of real-valued constellations corrupted by interferences—the Alamouti-SAIC/MAIC concept," *IEEE Trans. Signal Process.,* vol. 59, no. 7, pp. 3339–3354, July 2011.
[19] R. Meyer, W. H. Gerstacker, F. Obernosterer, M. A. Ruder, and R. Schober, "Efficient receivers for GSM MUROS downlink transmission," in *Proc. 2009 IEEE Pers. Indoor and Mob. Radio Commun.*, pp. 2399–2403.
[20] J. C. Olivier and W. Kleynhans, "Single antenna interference cancellation for synchronised GSM networks using a widely linear receiver," *IET Commun.*, vol. 1, no. 1, pp. 131–136, Feb. 2007.
[21] S. Badri-Hoeher, P. A. Hoeher, and W. Xu, "Single antenna interference cancellation (SAIC) for cellular TDMA networks by means of decoupled linear filtering/nonlinear detection," in *Proc. 2006 IEEE Int. Symp. on Pers. Indoor and Mob. Radio Commun.*, pp. 1–5.
[22] V. Bril, P. S. R. Niniz, and R. D. Vieira, "Advanced downlink receivers for GERAN," in *Proc. 2006 Int. Telecommunications Symposium*, pp. 443–448.
[23] L. Matellini, "Single antenna interference cancellation for GSM by enhanced maximum SNR filter," in *Proc. 2005 IEEE Int. Symp. on Wireless Commun. Syst.*, pp. 332–336.
[24] S. Verdù, *Multiuser Detection*. Cambridge University Press, 1998.
[25] W. Etten, "Maximum likelihood receiver for multiple channel transmission systems," *IEEE Trans. Commun.*, vol. 24, no. 2, pp. 276–283, Feb. 1976.
[26] P. A. Ranta, A. Hottinen, and Z. C. Honkasalo, "Co-channel interference cancellation receiver for TDMA mobile systems," in *Proc. 1995 IEEE Int. Conf. on Commun.*, pp. 17–21.
[27] J. T. Chen, J. W. Liang, H. S. Tsai, and Y. K. Chen, "Low-complexity joint MLSE receiver in the presence of CCI," *IEEE Commun. Lett.*, vol. 2, no. 5, pp. 125–127, May 1998.
[28] J. Zhang, A. M. Sayeed, and B. D. Van Veen, "Reduced-state MIMO sequence detection with application to EDGE systems," *IEEE Trans. Wireless Commun.*, vol. 4, no. 3, pp. 1040–1049, May 2005.
[29] M. O. Hasna, M. S. Alouini, A. Bastami, and E. S. Ebbini, "Performance analysis of cellular mobile systems with successive co-channel interference cancellation," *IEEE Trans. Wireless Commun.*, vol. 2, no. 1, pp. 29–40, Jan. 2003.
[30] D. Molteni, M. Nicoli, and M. Saily, "Resource allocation algorithm for GSM-OSC cellular systems," in *Proc. 2011 IEEE Int. Conf. on Commun.*, pp. 1–6.
[31] J. Penttinen, F. Calabrese, L. Maestro, K. Niemelä, D. Valerdi, and M. Molina, "Capacity gain estimation for orthogonal sub channel," in *Proc. 2010 Int. Conf. Wireless and Mob. Commun.*, pp. 62–67.
[32] M. A. Ruder, R. Schober, and W. H. Gerstacker, "Cramer-Rao lower bound for channel estimation in a MUROS/VAMOS downlink transmission," in *Proc. 2011 IEEE Pers. Indoor Mob. Radio Commun.*, pp. 1438–1442.
[33] D. Molteni and M. Nicoli, "A novel uplink receiver for GSM/EDGE systems with orthogonal sub channel feature," in *Proc. 2009 IEEE Asilomar Conf. on Sig., Syst., and Comput.*, pp. 977–981.
[34] 3GPP TS 45.003 v9.0, "Channel coding," 3GPP GERAN, Dec. 2009.
[35] M. Nicoli and U. Spagnolini, "Reduced-rank channel estimation for time-slotted mobile communication systems," *IEEE Trans. Signal Process.*, vol. 53, no. 3, pp. 926–944, Mar. 2005.
[36] D. Boss, T. Petermann, and K. Kammeyer, "Impact of blind versus non-blind channel estimation on the BER performance of GSM receivers," in *Proc. 1997 IEEE Signal Processing Workshop on Higher-Order Statistics*, pp. 62–67.
[37] S. Haykin, *Adaptive Filter Theory*, 4th edition. Prentice Hall, 2001.
[38] G. D. Forney, "Maximum-likelihood sequence estimation of digital sequences in the presence of intersymbol interference," *IEEE Trans. Inf. Theory,* vol. 18, no. 3, pp. 363–378, May 1972.
[39] W. H. Gerstacker and R. Schober, "Equalization concepts for EDGE," *IEEE Trans. Wireless Commun.*, vol. 1, no. 1, pp. 190–199, Jan. 2002.
[40] G. Zimmermann and W. Rupprecht, "Soft-decision output at sequential detection algorithms in digital mobile radio systems," in *Proc. 1994 IEEE Vehic. Tech. Conf. – Spring*, vol. 1, pp. 292–296.
[41] S. Brink, "Convergence behavior of iteratively decoded parallel concatenated codes," *IEEE Trans. Commun.*, vol. 49, no. 10, pp. 1727–1737, Oct. 2001.
[42] A. Goldsmith, *Wireless Communications*. Cambridge University Press, 2005.
[43] GP-080173, "Proposed proceeding on MUROS, WI rapporteur," 3GPP GERAN#37, Seoul, South Korea, Feb. 2008.
[44] P. Stoica and R. L. Moses, *Spectral Analysis of Signals*. Prentice Hall, 2005.
[45] R. E. Prieto, "A general solution to the maximization of the multidimensional generalized Rayleigh quotient used in linear discriminant analysis for signal classification," in *Proc. 2003 IEEE Int. Conf. on Acoustics, Speech, and Sig. Proc.*, vol. 6, pp. 157–60.
[46] X. Wang and H. V. Poor, "Space-time multi-user detection in multipath CDMA channels," *IEEE Trans. Signal Process.*, vol. 47, pp. 2356–2374, Sept. 1999.

Daniele Molteni received the M.Sc. in Telecommunication Engineering (with honors) in 2007 and the Ph.D. in Information Technology in 2011 at Politecnico di Milano, Italy. During 2011 he joined Nokia Siemens Networks (Helsinki, Finland) as intern researcher to investigate receiving algorithms and scheduling strategies for GSM/EDGE Voice Evolution scenarios. He is currently working at Schlumberger Gould Research center (Cambridge, UK) dealing with fiber optic sensing technology. His research interests focus on signal processing topics for wireless communications and seismic exploration. In particular, he has been working on resource allocation algorithms for multi-cell OFDMA and TDMA systems, sensors networks and distributed monitoring systems.

Monica Nicoli received the M.Sc. degree (with honors) and the Ph.D. degree in Telecommunication Engineering from Politecnico di Milano, Italy, in 1998 and 2002, respectively. In 2001, she was visiting researcher at Uppsala University, Sweden. Since 2002, she has been with Dipartimento di Elettronica, Informazione e Bioingegneria, Politecnico di Milano, where she is an Assistant Professor. Her research interests are in the area of signal processing for wireless communication systems, with emphasis on PHY layer algorithms, distributed and cooperative systems, wireless positioning and intelligent transportation systems. She is Associate Editor for the *EURASIP Journal on Wireless Communications and Networking* and she served as Lead Guest Editor for the special issue on Localization in Mobile Wireless and Sensor Networks. She received the Marisa Bellisario Award in 1999.